This work was carried out in whole or in part within the framework of the NOMATEN Center of Excellence, supported from the European Union Horizon 2020 research and innovation programme (Grant Agreement No. 857470) and from the European Regional Development Fund via the Foundation for Polish Science International Research Agenda PLUS programme (Grant No. MAB PLUS/2018/8).

This is a copy of the publication which appeared in Materials Science in Semiconductor Processing, Volume 165, October 2023, 107640, published on: 7 June 2023.

DOI: 10.1016/j.mssp.2023.107640

Materials Science in Semiconductor Processing 165 (2023) 107640

Contents lists available at ScienceDirect

Materials Science in Semiconductor Processing

journal homepage: www.elsevier.com/locate/mssp

Depth-distribution of resistivity within ion-irradiated semiconductor layers revealed by low-kV scanning electron microscopy

I. Jóźwik [a,b,*], J. Jagielski [a,c], P. Ciepielewski [a,d], E. Dumiszewska [a], K. Piętak-Jurczak [a,e,f], M. Kamiński [a,g], U. Kentsch [h]

[a] Lukasiewicz Research Network, Institute of Microelectronics and Photonics, Al. Lotników 32/46, Warsaw, Poland
[b] NOMATEN CoE, NOMATEN MAB+, National Centre for Nuclear Research, 7th A. Soltana Str., 05-400, Świerk, Otwock, Poland
[c] National Centre for Nuclear Research, Department of Material Physics, 7th A. Soltana Str., 05-400, Świerk, Otwock, Poland
[d] Polish Academy of Science, Institute of Physics, Al Lotnikow 32-46, PL-02668, Warsaw, Poland
[e] Warsaw University of Technology, Faculty of Chemistry, Nowakowskiego 3, 00-664, Warsaw, Poland
[f] Warsaw University of Technology, Doctoral School No 1, Plac Politechniki 1, 00-661, Warsaw, Poland
[g] Warsaw University of Technology, Institute of Microelectronics and Optoelectronics, Pl. Politechniki 1, 00-661, Warsaw, Poland
[h] Institute of Ion Beam Physics and Materials Research, Helmholtz-Zentrum Dresden-Rossendorf e.V. (HZDR), D-01328, Dresden, Germany

ARTICLE INFO

Keywords:
AIIIBV
Ion damage
Low-kV SEM

ABSTRACT

Low-kV scanning electron microscopy imaging was used to visualize the 2D profiles of internal resistivity distribution in 600 keV He^{2+} ion-irradiated epitaxial GaAs and $Al_{(0.55)}Ga_{(0.45)}As$. The influence of the dopant concentration on DIVA (damage-induced voltage alteration) contrast formation has been studied in this paper. The threshold irradiation fluencies (the fluencies below which no damage-related contrast is observed) were defined for each studied material. The results show that the same level of damage in the material caused by ion irradiation becomes visible at lower threshold fluence in the case of lower-doped sample of the same composition. The aluminum content in the composition of materials exposed to ion irradiation and subsequent DIVA contrast formation mechanism was considered as well. The carrier concentration in irradiated layers has been studied by Raman spectroscopy and photoluminescence measurements, which confirmed that the increase of the resistivity of the material caused by ion-irradiation damage generation is resulting from the formation of deep states in the bandgap trapping free carriers.

1. Introduction

One of the essential processes used currently for the production of modern compound AIIIBV semiconductor devices is ion implantation that has two major applications: doping and electrical isolation. The former, followed by an annealing process, is to establish proper p- or n-type conductivity, the latter is to convert a doped layer into a highly resistive one, and is called implantation induced isolation, implant isolation either isolation by ion irradiation [1–5]. It is commonly accepted that isolation is driven by trapping of carriers at deep energy levels in the forbidden band gap associated to the radiation induced defects or to specific impurities used for the implantation. It is worth to recall that the term "*implantation*" is used when the ion beam is used for doping with given impurity atoms, while "*irradiation*" is used when the sole purpose of the beam is to deposit energy in the material. The common technique of visualization of resistive parts of the irradiated semiconductor structure area in order to confirm that electrical insulation has been effectively obtained is wet selective etching development over the cleaved structure (where the etch stops on the border of conductive - nonconductive material) followed by subsequent scanning electron microscopy (SEM) imaging. Among other drawbacks of this technique, such as time consumption and complex preparation leading to imprecise results, the most important is that the method can be applied only to selected materials which do follow the etch-stop rule.

Our previous papers [6–9] show that the efficient and easy-to-apply technique of the visualization of the highly resistive isolated regions in semiconductors is a unique DIVA (Damage-Induced Voltage Alteration) contrast imaging by means of low- and ultra-low kV scanning electron microscopy (SEM). The DIVA contrast is based on the altered SE (secondary electrons) emission/detection from the semiconductor surface

* Corresponding author. Institute of Microelectronics and Photonics, Wólczyńska 133, 01-919, Warsaw, Poland.
E-mail address: iwona.jozwik@imif.lukasiewicz.gov.pl (I. Jóźwik).

https://doi.org/10.1016/j.mssp.2023.107640
Received 16 March 2023; Received in revised form 13 May 2023; Accepted 29 May 2023
Available online 7 June 2023

which local electrical potential has been modified during primary electron bombardment in the result of increase of ion-damaged-induced resistivity. The contrast development in each particular case is dependent on the SEM imaging conditions, such as electron beam energy or dwell time. In another words, the same material irradiated with energetic ions may appear in a different way depending on the electron beam parameters and scanning method. The unique feature of DIVA contrast imaging is that it enables to visualize directly the damage-induced resistivity changes or even damage distribution within the surface layer if analysis is made on cleaved samples. In particular, not only is DIVA bringing information about the size of the ion-damaged/resistant zone in the cross section of the semiconductor layer, but also provides information on the development of internal resistivity of the layer along the way of penetrating ions. In this paper we will present a deeper insight into DIVA contrast mechanism taking into account such parameters as dopant concentration and aluminum (Al) content in the semiconductors subjected to irradiation with certain ions.

2. Materials and methods

Semi-insulating GaAs wafers of (100) orientation were used as supports to grow 2 – 4 micron-thick epitaxial layers of GaAs and AlGaAs using MOCVD (metalorganic chemical vapor deposition) reactor. During the growth the epilayers were intentionally n-doped (Si) to various concentrations (see Table 1). The dopant concentration in epilayers was determined by the Electrochemical Capacitance-Voltage profiling (ECV) method [10]. After the growth, each wafer was cut into 6 pieces which were subsequently irradiated at room temperature with fluencies in the range of 5e12 to 5e14 cm^{-2} of He^{2+} at 600 keV (with one sample of each material left unirradiated as a reference sample) using an air insulated 500 kV ion implanter (High Voltage Engineering) at Helmholtz-Zentrum Dresden-Rossendorf. The ion irradiations were performed at room temperature with 7° tilt from the normal to the sample surface to avoid channeling. The freshly cleaved cross-sections of irradiated samples were subjected to low-kV SEM imaging using Auriga CrossBeam Workstation (Carl Zeiss) equipped with the unique in-lens SE detector (true SE1) at low energy operation (0.5 keV). Room temperature Raman measurements on GaAs samples were performed on Renishaw inVia Raman Microscope using Nd:YAG laser (532 nm). The measurements were performed with laser focused on (100) surface of GaAs sample using x100 objective and numerical aperture NA = 0.9 in backscattering geometry.

3. Results and discussion

3.1. *Influence of semiconductor doping level on the image contrast formation*

Figs. 1 and 2 present the low-kV SEM images of the cross-sections of ion-irradiated samples of GaAs and AlGaAs. The contrasts in the images shown in Figs. 1 and 2 develop along the irradiation direction of the He^{2+} ions and present fluence-dependent character. At certain imaging conditions (here 0.5 keV of primary electron beam) this contrast appears first as darkening in the end of irradiated zone image, which further spreads over the whole irradiation depth to finally become bright at specified ion fluence. The fluence for which the ion-irradiation damage-related contrast becomes visible is hereafter called a threshold fluence. Below the threshold fluence no signs of DIVA contrast are observed. In other words, the threshold fluence is the minimum fluence which converts a conductive layer into a resistive one at the level which affects the image of a studied material at selected SEM imaging conditions.

Table 1
Samples used in the study.

Sample name	Material	Dopant	Dopant concentration [cm^{-3}]	Type
low-doped GaAs	GaAs	Si	4.2e17	n
highly-doped GaAs	GaAs	Si	8.3e18	n
low-doped AlGaAs	$Al_{(0.55)}Ga_{(0.45)}As$	Si	4.6e17	n
highly-doped AlGaAs	$Al_{(0.55)}Ga_{(0.45)}As$	Si	1.3e18	n

As it has been presented in our previous papers [6–9], the DIVA contrast is based on the charging effect occurring during SEM imaging of the semiconducting material that has been converted into highly resistive one in the outcome of energetic ions irradiation and resultant damage. The electrical potential induced during electron bombardment of the sample surface has an impact on the secondary electron (SE) yield either SE collection efficiency. Depending on the level of damage at particular depth of the sample and imaging conditions, the image appears either dark or bright, which is directly dependent on the local resistivity of the sample at specified place.

Basing on our previous findings [7,8], the darkening of the image at 0.5 keV imaging conditions can be interpreted as the positive charging of the sample surface, while brightening observed with the increase of the ion fluence is the result of negative potential on the surface. The comparison of individual images registered for all studied materials shows clearly, that for a specific material (e.g. GaAs) the damage visibility depends not only on the ion fluence, but also the dopant concentration (compare for example pairs of images c and i in Fig. 1or Fig. 2).

It is commonly known that the elastic scattering of helium ions within the material leads to the formation of damage zones. The level of generated damage and its distribution along the primary direction of incoming ions can be calculated using SRIM code [11] and depends on the material composition, but is insensitive to the dopant concentration of the semiconductor. Despite the fact, that the level and in-depth distribution of damage are the same in both, low- and highly-doped GaAs samples irradiated with the same fluence of 600 keV He^{2+} ions, the evolution of image contrast with depth differs much: the damage-related contrast appears first as a dark narrow line at the very end of the epilayer in image of low-doped GaAs sample (Fig. 1 b) at fluence 5e12 cm^{-2}, while the heavily-doped GaAs is found to be practically insensitive to this ion fluence, as no contrast is observed in the SEM image (Fig. 1 h). It seems thus that the same level of damage becomes visible much sooner (lower threshold fluence) in the case of low-doped sample. The dependence of contrast appearance on the dopant concentration is even more pronounced with the accumulation of fluence (compare Fig. 1 c and i or Fig. 1 d and j, as an example). Interestingly, the contrast distribution appears similar for highly-doped sample at the threshold fluence of 2e13 cm^{-2} as for low-doped GaAs at 5e12 cm^{-2} fluence of He^{2+} ions.

For studied AlGaAs the first symptoms of the damage visibility in SEM within the epilayer appear at a fluence of 5e12 cm^{-2} in low-doped sample (dark line in Fig. 2 b). At the fluence of 2e13 cm^{-2}, which is a threshold fluence for highly-doped sample, the differences in the contrast appearance with respect to the doping level become more prominent (Fig. 2 c and i). With the increase of the ion fluence to 5e13 cm^{-2} the images of both samples (low- and highly-doped) become similar in terms of the image contrast distribution along the ion irradiation direction. The dark contrast is slightly evolving/broadening toward the sample surface with the fluence increase (Fig. 2 d and j), turning into brightening of the end of damage zone at the 2e14 cm^{-2} (Fig. 2 e and k) to finally form bright contrast overall the irradiated zone at the highest fluence (Fig. 2 f and l).

Fig. 3 presents the depth evolution of normalized signal intensity measured along the ion irradiation direction, with the sample surface set at x = 0 for both studied materials (GaAs and AlGaAs). The straight lines in both images (Fig. 3 a and b) represent the normalized signals registered at the threshold fluence for low-doped samples (5e12 cm^{-2}, as shown above), while the dash-dotted lines are assigned to highly-doped samples of each material in the same irradiating conditions. The purpose of this comparison is to express semi-quantitatively the measure of the

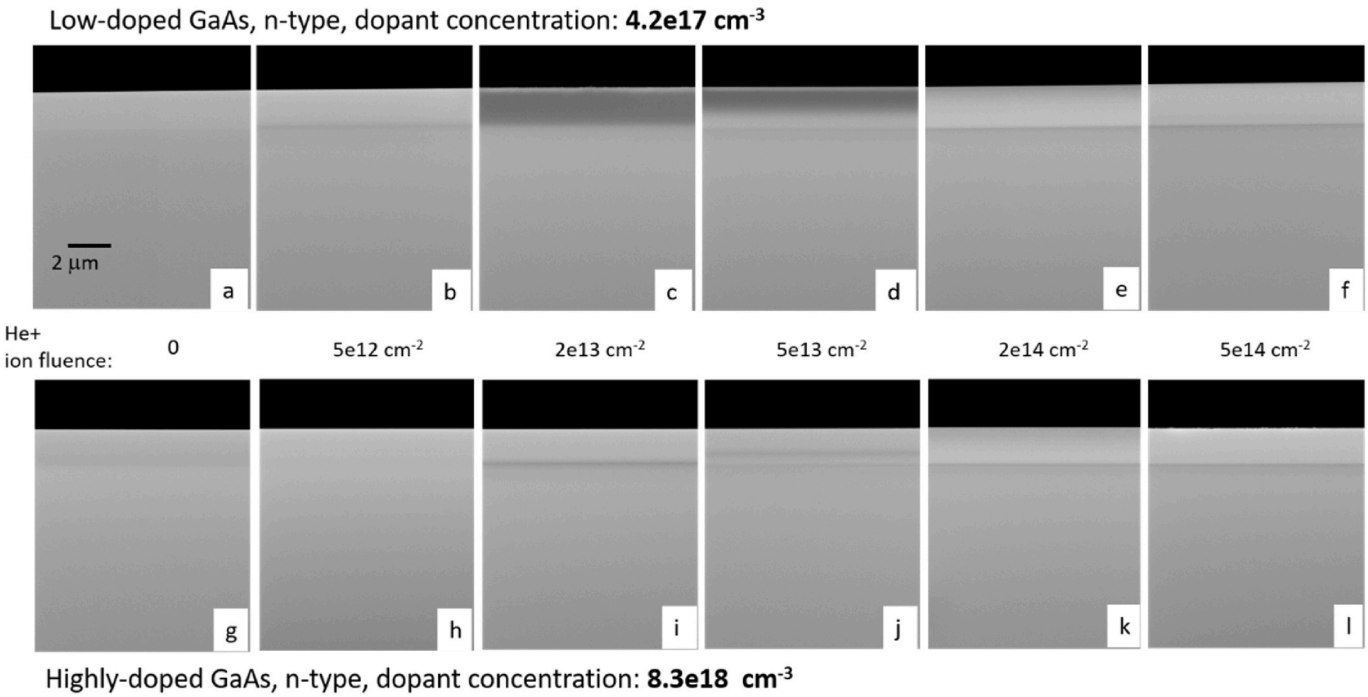

Fig. 1. Low-kV SEM cross-section images of virgin and ion-irradiated GaAs with different dopant concentrations: 4.2e17 cm^{-3} (a–f) and 8.3e18 cm^{-3} (g–l).

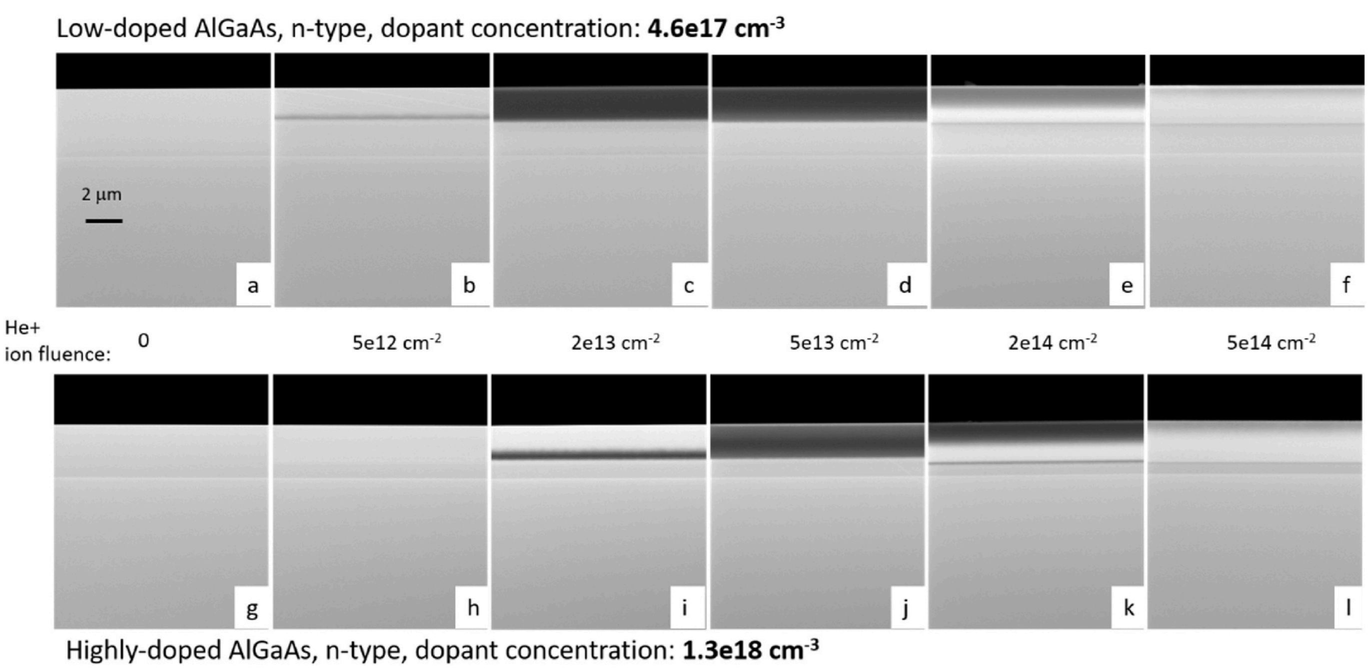

Fig. 2. Low-kV SEM cross-section images of virgin and ion-irradiated AlGaAs with different dopant concentrations: 4.6e17 cm^{-3} (a–f) and 1.3e18 cm^{-3} (g–l).

dependence of the response of each studied composition to the doping level at specified irradiation fluence.

The overlay in each image in Fig. 3 shows the damage distribution peak calculated by SRIM code for GaAs and $Al_{(0.55)}Ga_{(0.45)}As$. The damage generated on the way of He^{2+} ions slowing down within the epilayer is not homogenous, but it evolves along the ion irradiation direction, starting from the sample surface towards the bulk. This distribution is usually referred to as the Bragg peak. The specific level of damage turns into the increase of local resistivity of the material by the mechanism of conductivity compensation [1,12]. The resulting local differences in the surface potential within the two-dimensional irradiation layer affect the trajectories of secondary electrons emitted from the sample, which in turn leads to alteration of signal intensity registered by the SE in-lens detector. The in-lens detection allows selective collection of secondary electrons type 1 (SE1) which carry information about the electrical properties of studied material.

A careful analysis of data in Fig. 3, however, shows that the maximum of damage distribution peak does not correspond to the minimum value of normalized signal intensity neither for GaAs nor AlGaAs low-doped samples. The misfit between the Bragg peaks maxima and normalized signal intensity minima in studied cases (Fig. 3) is related to the fact, that the DIVA contrast development is not linear, i.e.

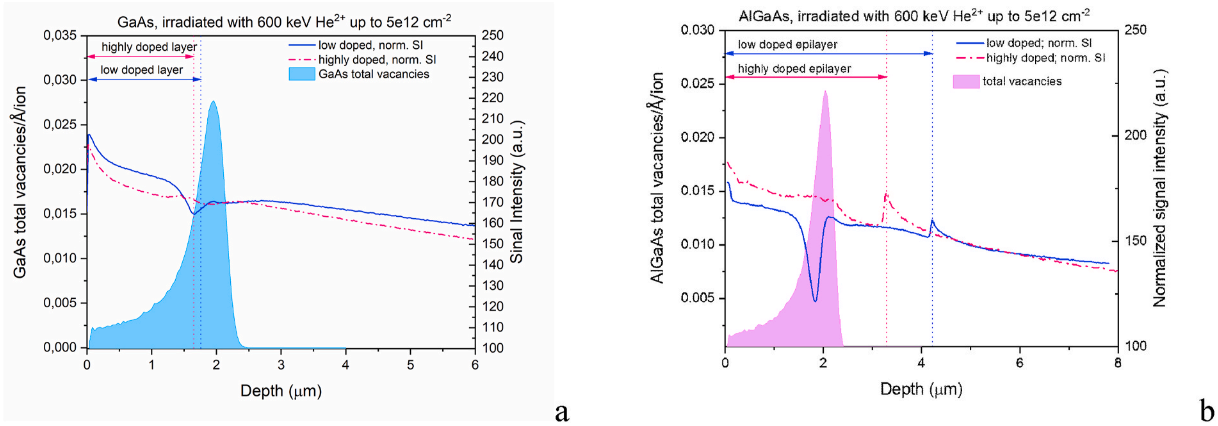

Fig. 3. (color online) SEM signal intensity profiles over the cross-sections of GaAs (a) and AlGaAs (b) irradiated with He^{2+} ion up to 5e12 cm^{-2}. The overlay of damage (total vacancies) distribution peak calculated by SRIM code is presented for each material.

the image darkening does not necessarily occurs at the depth of the highest damage. The important to note is that the main mechanism of the DIVA contrast development is based on the relative changes in the surface electrical potential. As is has been shown previously, the image appearance of damaged zone greatly depends on the SEM imaging conditions [8]. There are many factors driving the contrast development in ion-irradiated zone in semiconductors, some of them are local resistivity induced by damage, doping concentration and electron beam parameters, such as primary energy and current density. The contrast is not providing the information quantitatively, however. For a fixed ion fluence and imaging conditions a more pronounced effect of an increase in epilayer resistivity occurs in samples of lower original carrier concentration. The DIVA contrast and signal intensity profiles of the registered images are tightly related to the internal resistivity of the sample after the irradiation. According to SRIM simulations, the damage distributed within the ion-irradiated layer depends on the material composition, not on doping type/level. Fig. 3 (and also Figs. 1–2) clearly presents the differences in the DIVA contrast development underneath the irradiated sample surface, depending on the dopant concentration: the higher the dopant concentration, the higher the threshold fluence at which the DIVA contrast develops in SEM image. This might be considered as a drawback, as the visualization of damaged zone does not depend only on the material composition, but also on doping level. However, on the other hand, by low-kV imaging one is able to estimate the fluence at which implant isolation is effective for a specific dopant concentration. According to Boudinov et al. [13] the fluences which turn the conductive p- or n-type layer into insulating ones are <1e14 cm^{-2} in case of light ions (such as H^+, He^+, B^+, O^+) as for each ion tens or hundreds of carriers are removed. Assuming, that the dark contrast (at 0.5 kV SEM imaging specifically) spreading over the entire depth of the irradiated layer can be interpreted as the satisfactory resistivity obtained throughout the whole irradiated layer thickness, one can indicate the effective fluence value by comparative analysis of the images collected at the samples cross sections using DIVA contrast imaging. In case of the studied AlGaAs, the estimated values assuring that the resistivity has been achieved within the whole depth of irradiated zone would be 2e13 cm^{-2} and 5e13 cm^{-2} for low-doped and highly-doped samples, respectively (see Fig. 2 c and j).

The influence of the doping level on DIVA contrast mechanism has been studied also for p-type GaAs and n-type InAlP. For the sake of clarity the results of low-kV imaging are presented in Fig. 1S and 2S in the Supplementary materials.

3.2. Influence of the Al content on DIVA contrast

One of the factors worth considering is the Aluminum content on DIVA contrast formation. According to van Lippen et al. [16]. the threshold fluence to convert a conductive layer into a highly resistive one and the thermal stability of the AlGaAs layer does not depend on the Al content. Lippen shows that the defects responsible for the free carrier trapping are special kinds of defects, very stable at room temperature. The natural candidates with these characteristics are antisite defects or complexes.

As measured, the values of doping level of low-doped n-type GaAs and AlGaAs studied in this work are similar, i.e. 4.2e17 cm^{-3} and 4.6e17 cm^{-3}, respectively. The comparison of the images a – c from Fig. 1 with their analogues from Fig. 2 seems to confirm the finding of Lippen, that the resistivity does not depend on the Al content, which is very nicely confirmed by the evolution of DIVA contrast directly connected to the resistivity distribution within the irradiated layer. In both studied materials the contrast is developing in the same way, for each fluence up to 2e13 cm^{-2}. However, by comparing Fig. 1 d with Fig. 2 d a difference in the image contrast registered in low-kV can be observed. The AlGaAs irradiated up to 5e13 cm^{-2} appears dark over the whole depth of damage zone (Fig. 2 d), while GaAs sample (of the same doping level) irradiated at the same conditions starts to turn bright at the very end of the irradiated depth (Fig. 1 d). Similarly, low-kV SEM contrast in the image of GaAs irradiated with 2e14 cm^{-2} evolves much faster (totally bright contrast over the whole irradiated layer, Fig. 1e) than the AlGaAs in the same conditions (brightening only at the end of the irradiated zone, Fig. 2 e). According to considerations presented formerly [7,8] and above in this paper one can conclude, that the He^{2+} irradiation to the same fluence (but with values above 2e13 cm^{-2} in studied cases) leads to higher resistivity of GaAs layer in comparison to AlGaAs, which proves that the Al content has an impact on the electrical properties of the material after ion irradiation, when compared to GaAs. This is again a clear evidence, that DIVA is a nice tool to directly visualize the sample resistivity related to ion irradiation, however it is not a method suitable for quantitative characterization of level of damage, as the contrast depends on many factors, which are (among others) Al content, dopant concentration and imaging conditions, which one must keep in mind.

3.3. Raman spectroscopy analysis of irradiated GaAs

The mechanism responsible for increase of the local resistivity of the material in the result of ion irradiation damage is tightly bound with the formation of deep states in the bandgap trapping free carriers. Raman spectroscopy studies on the highly-doped GaAs sample clearly confirm this finding. In the applied configuration of measurement, only LO Raman mode is active for undoped samples. In our case the GaAs epilayer was heavily n-doped with Si (8.3e18 cm^{-3}). The electron plasma couples with LO phonon creating LO-plasmon modes L+ and L- observed in the Raman spectra of unirradiated and low-fluence (i.e. from 0 to 2e13 cm^{-2}) irradiated highly-doped GaAs samples. Carriers concentration obtained from the L+ plasmon-phonon modes energies give (according to [14]) the values of 7.3e18, 5.8e18 and 5.2e18 cm^{-3}, respective to increasing ion fluence. The presence of the LO mode observed in these irradiated samples is most likely related to the depletion layer present on their surfaces (see Fig. 4). Further ion fluence accumulation leads to the L+ and L- phonon-plasmon modes disappearance, which indicates that the concentration of free carriers (electrons) falls below 5e17 cm^{-3} when fluence of irradiation exceeds 5e13 cm^{-2} [14,15]. Later on only LO mode is present in the Raman spectra, however the small shoulder of TO mode has been also observed, which probably results from some misalignments in the experimental configuration or imperfections on the sample surface.

Additionally to Raman spectra, the room temperature inter-band photoluminescence (PL) spectra were measured in the same set-up configuration. The results presented in Fig. 5 clearly demonstrate that with the increase of ion-irradiation fluence, the intensity of photoluminescence is gradually damping, to disappear completely at the fluence of 2e14 cm^{-2}. The irradiation of GaAs with He^{2+} ions leads to generation of increasing number of defects which (most likely) introduce deep states in the GaAs band gap, which trap free electrons from the donor. The decreasing number of free carriers (electrons) is manifested in the Raman spectra and simultaneously damp the inter-band photoluminescence by creating effective channel of nonradiative decay from conduction to valence band. It should be noted, however, that the Raman spectra analysis presented above brings the information on the total carrier concentration within the probed depth of material, contrary to the resistivity profiling by DIVA contrast. Nevertheless this technique proves that the mechanism of resistivity increase is tightly bound to free carrier trapping due to the ion-irradiation induced damage formation.

4. Summary and conclusions

The current studies show deeper insight in damage-induced voltage alteration (DIVA) contrast development mechanism used for ion-induced resistivity distribution imaging in irradiated GaAs and AlGaAs. The influence of the doping concentration of the semiconducting material has been considered as one of the factors driving the DIVA contrast mechanism formation. The analysis of image signal intensity profiles with irradiation damage accumulation for specific doping level in the studied GaAs and AlGaAs samples has been presented

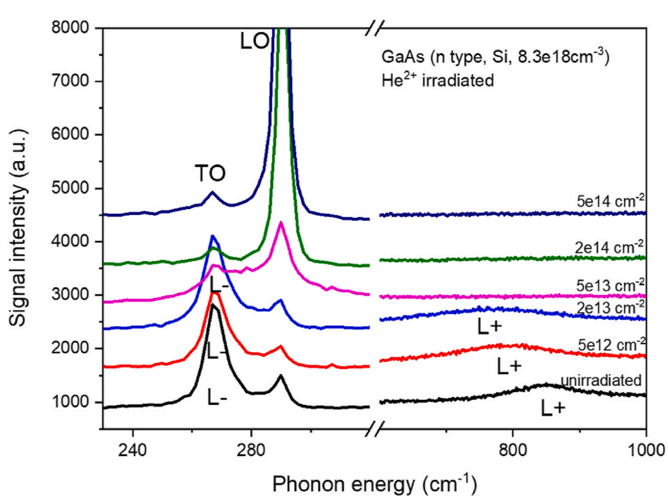

Fig. 4. (color online) The Raman spectra of n-GaAs samples (Si donor concentration 8.3e18 cm^{-3}) irradiated with increasing fluencies of He^{2+} ions. LO phonon mode and coupled LO phonon-plasmon modes L+,L- are observed. (see detailed explanation in the text).

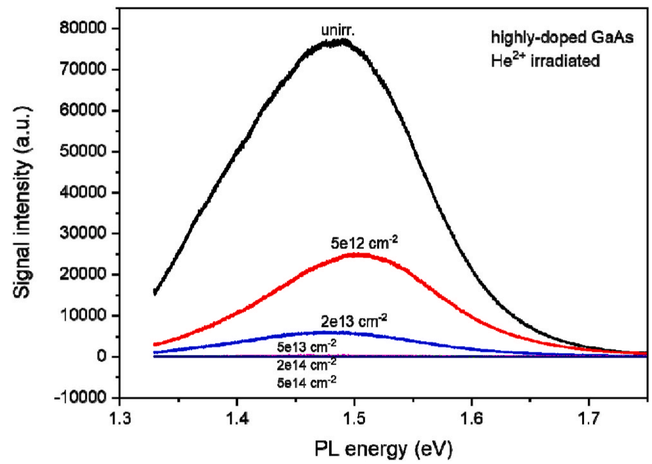

Fig. 5. The room temperature inter-band PL spectra of highly-doped n-GaAs samples (Si donor concentration 8.3e18 cm^{-3}), unirradiated and irradiated with increasing fluence of He^{2+} ions.

and supported with Raman spectroscopy and photoluminescence measurements. For a specified initial dopant concentration (which has an impact on the free carrier concentration), the effective mobility of carriers deteriorates in a consequence of ion irradiation. The decrease of effective free carrier concentration with the accumulation of radiation damage is a clear evidence of carrier removal via capture at the trapping centers. For each studied composition, the threshold fluence for contrast formation has been determined. On the basis of studies we can conclude, that the higher the dopant concentration, the higher the accumulation fluence responsible for the contrast appearance under electron bombardment. Additionally, the Aluminum content has been considered as a natural factor influencing the DIVA contrast formation. The studies showed that the response of the studied materials in terms of resistivity achieved by implant isolation technique for specified irradiation conditions depends on the Al content: for ion fluencies above 2e13 cm^{-2} the increase of the low-kV image contrast related to local resistivity develops faster for the Al-free material.

The results of the study presented in this paper once again proved DIVA contrast imaging as an easy, fast and reliable method of direct visualization of the internal resistivity distribution of ion-irradiated semiconductors in two dimension. The mechanism of contrast formation based on the charging effect in low-kV SEM is sensitive to the local resistivity changes within the ion-damaged layer/zone of material. The contrast provides the information on local changes in the sample resistivity, not the level of damage, and depends on various factors including the SEM imaging conditions due to the multi-factor-character of the mechanism laying behind the contrast generation it cannot be treated quantitatively. Nevertheless, optimizing the electron beam imaging conditions allows one to obtain directly the two-dimensional image of the ion-irradiated zone of the material, which may be very helpful in verification of the localization and continuity of the implant isolation during semiconductor processing and device fabrication.

CRediT authorship contribution statement

I. Jóźwik: Writing – original draft, Visualization, Methodology, Investigation, Data curation, Conceptualization. **J. Jagielski:** Writing – original draft. **P. Ciepielewski:** Writing – review & editing, Resources, Data curation. **E. Dumiszewska:** Writing – review & editing, Resources. **K. Piętak-Jurczak:** Writing – review & editing, Resources, Data curation. **M. Kamiński:** Writing – review & editing, Resources. **U. Kentsch:** Writing – review & editing, Resources.

Declaration of competing interest

The authors declare that they have no known competing financial interests or personal relationships that could have appeared to influence the work reported in this paper.

Data availability

Data will be made available on request.

Acknowledgment

This work has been financed by the National Science Centre, Poland, under the grant number 2017/27/B/ST8/01158. I.Jóźwik acknowledges support by RADIATE project under the Grant Agreement 824096 from the EU Research and Innovation program HORIZON 2020, and the support from the European Regional Development Fund via the Foundation for Polish Science International Research Agenda Plus program grant no. MAB PLUS/2018/8 which partially covered her salary during preparation of this article. Parts of this research were carried out at IBC at the Helmholtz-Zentrum Dresden - Rossendorf e. V., a member of the Helmholtz Association. We would like to thank Franziska Nierobisch and Stefan Eisenwinder for assistance. K. Piętak-Jurczak acknowledges financial support from IDUB project (Scholarship Plus programme).

Appendix A. Supplementary data

Supplementary data to this article can be found online at https://doi.org/10.1016/j.mssp.2023.107640.

References

[1] S.J. Pearton, Ion implantation for isolation of III-V semiconductors, Mater. Sci. Rep. 4 (1990) 313–363, https://doi.org/10.1016/S0920-2307(05)80001-5.

[2] J.P. Donnelly, The electrical characteristics of ion implanted compound semiconductors, Nucl. Instrum. Methods 182/183 (1981) 553–571, https://doi.org/10.1016/0029-554X(81)90777-1.

[3] G. Hanington, Y.M. Hsin, Q.Z. Liu, P.M. Asbeck, S.S. Lau, M. Asif Khan, J.W. Yang, Q. Chen, P/He ion implant isolation technology for AlGaN/GaN HFETs, Electron. Lett. 34 (2) (1998) 193–195, https://doi.org/10.1049/el:19980091.

[4] L.N. Large, R.W. Bicknell, Ion-implantation doping of semiconductors, J. Mater. Sci. 2 (1967) 589–609, https://doi.org/10.1007/BF00752224.

[5] B.J. Sealy, Ion implantation doping of semiconductors, Int. Mater. Rev. 33 (1) (1988) 38–52, https://doi.org/10.1179/imr.1988.33.1.38, 1988.

[6] I. Jóźwik, E. Dąbrowska, A. Maląg, A. Barcz, Direct imaging of irradiation damage in semiconductors by low-energy SEM, ECS Journal of Solid State Science and Technology 6 (7) (2017) 415–417, https://doi.org/10.1149/2.0191707jss.

[7] Iwona Jóźwik, Barcz Adam, Elżbieta Dąbrowska, Ewa Dumiszewska, Paweł Piotr Michałowski, Damage-induced voltage alteration (DIVA) contrast in SEM images of ion-irradiated semiconductors, Ultramicroscopy 204 (2019) 6–9, https://doi.org/10.1016/j.ultramic.2019.04.013.

[8] I. Jóźwik, J. Jagielski, E. Dumiszewska, M. Kamiński, U. Kentsch, Resistivity contrast imaging in semiconductor structures using ultra-low energy scanning electron microscopy, Ultramicroscopy 228 (2021), 113333, https://doi.org/10.1016/j.ultramic.2021.113333.

[9] Iwona Jóźwik, Jacek Jagielski, Piotr Caban, Maciej Kamiński, Kentsch Ulrich, Direct visualization of highly resistive areas in GaN by means of low-voltage scanning electron microscopy, Mater. Sci. Semicond. Process. 138 (2022), 106293, https://doi.org/10.1016/j.mssp.2021.106293.

[10] J. Hilibrand, R.D. Gold, Determination of the impurity distribution in junction diodes from capacitance-voltage measurements, RCA Rev. 21 (1960) 245.

[11] J.F. Ziegler, J.P. Biersack, U. Littmark, The Stopping and Range of Ions in Solids, Pergamon, New York, 1985.

[12] V.N. Brudnyi, M.A. Krivov, Sov. Phys. J. 23 (1980) 45.

[13] H. Boudinov, A.V.P. Coelho, J.P. de Souza, Electrical isolation of *p*-type GaAs layers by ion irradiation, J. Appl. Phys. 91 (2002) 6585–6587, https://doi.org/10.1063/1.1469693.

[14] G. Absteriter, E. Bauser, A. Fischer, K. Ploog, Raman spectroscopy—a versatile tool for characterization of thin films and heterostructures of GaAs and AlGaAs, Appl. Phys. 16 (1978) 345–352.

[15] A. Wysmołek, D. Plantier, M. Potemski, T. Słupiński, Z.R. Żytkiewicz, Coupled plasmon–LO-phonon modes at high-magnetic fields, Phys. Rev. B 74 (2006), 165206.

[16] T.v. Lippen, H. Boudinov, H.H. Tan, C. Jagadish, Electrical isolation of AlxGa1−xAs by ion irradiation", Appl. Phys. Lett. 80 (2002) 264–266, https://doi.org/10.1063/1.1427422.